ChemComm

Cite this: *Chem. Commun.*, 2011, **47**, 4944–4946

www.rsc.org/chemcomm

COMMUNICATION

A novel mesoporous carbon–silica–titania nanocomposite as a high performance anode material in lithium ion batteries†

Yuanyuan Zhou,[a] Younghun Kim,[a] Changshin Jo,[b] Jinwoo Lee,[b] Chul Wee Lee[a] and Songhun Yoon*[a]

Received 27th January 2011, Accepted 1st March 2011
DOI: 10.1039/c1cc10539f

An ordered mesoporous carbon–silica–titania material was prepared using the tetra-constituents co-assembly method. As regards its anode performance in lithium ion batteries, the composite material anode exhibited a high capacity (875 mAh g^{-1}), a higher initial efficiency (56%) and an improved rate.

Ordered mesoporous carbon (OMC) composite materials containing electrochemically active metal oxides have been widely investigated for use as the anodes in lithium ion batteries (LIBs).[1] These nanostructured materials have been recognized as good anode candidates, because of their beneficial characteristics: (i) the short diffusion path of lithium ions within the nanosized pore walls, (ii) easy electrolyte penetration through the mesopores, and (iii) highly available charge storage sites due to the high surface area.[1,2] Typically, mesoporous nanocomposites of OMC with metal oxides such as CoO, SnO_2, NiO and TiO_2 have exhibited improved anode performances.[3,4] Especially, TiO_2 has an intrinsically low electrical conductivity ($\sim 10^{-12}$ S cm^{-1}), which can result in low rate capability and requires a highly-developed conductive percolation network for the conductivity to increase.[5] With this in mind, many researchers have tried to prepare carbon–TiO_2 composite materials.[4,5] Among them, an OMC–titania nanocomposite has been intensively investigated. When it was applied as the anode in LIBs, a reversible capacity of about 150–300 mAh g^{-1} was observed within the range of 1 to 3 V *vs.* Li/Li^+.[5] Furthermore, it has been reported that a highly crystalline TiO_2 phase formed after high temperature calcination above 400 °C, which resulted in a distinctive voltage plateau. This plateau represented a more ordered first-order phase transition from Li_xTiO_2 to $Li_{0.5}TiO_2$, which produced a cell volume increase of 4% and cycle fading.[5] To improve the cyclability, therefore, a less-developed crystalline phase of TiO_2 is preferable. Also, less-developed crystals show a sloped voltage profile, which is beneficial to the state of charge (SOC) prediction in LIBs.

While high reversible capacities ranging from 850 to 1100 mAh g^{-1} have been reported for the OMC anode itself, a low initial efficiency of about 30% was reported, which was attributed to the decomposition of the electrolyte on the carbon surface having a high surface area (>1500 m^2 g^{-1}).[6] A higher initial efficiency is required for the efficient utilization of the electrode as a charge storage device. Hence, a smaller surface area is desirable, while retaining ordered mesopores for fast electrolyte transport.

In order to prepare a mesoporous carbon nanocomposite with amorphous TiO_2, herein, a tetra-constituent co-assembly (Tetra-CCA) method using Ti–citrate precursor is developed. A block copolymer surfactant, oligomeric resol and silicate source are reacted with Ti–citrate solution.[7] Here, the silicate was added for the purpose of increasing the structural strength and forming a higher ordered structure.[7] After the preparation of the composite, its performance as the anode in lithium ion batteries is investigated. To the best of our knowledge, this is the first attempt to prepare a mesoporous carbon composite with amorphous titanate using the Tetra-CCA method and use it as the anode in a lithium ion battery.

The detailed synthesis procedure is included in the ESI† and described schematically in Fig. S1. As can be seen, the Tetra-CCA method was employed. Using evaporation-induced self-assembly (EISA), an ordered nanocomposite was obtained and polymerization was conducted. After carbonization, an ordered mesoporous carbon–silica–titania nanocomposite (m-CST) was obtained (see Fig. 1). The silica was removed by NaOH treatment, producing a mesoporous carbon–titania (m-CT).

In Fig. 2, the N_2 sorption isotherms for m-CST and m-CT are shown. Here, an increase in the volume of adsorbed N_2 was observed after NaOH etching. The pore size distributions (PSDs) of m-CST and m-CT are given in the inset. A monodispersed PSD was obtained in the case of m-CST with a size of 3.46 nm, but m-CT showed a bimodal PSD with sizes of 2.67 and 3.74 nm, which is similar to the result obtained by the tri-constituent co-assembly method.[7,8] The large pores of m-CST (3.46 nm) and m-CT (3.74 nm) corresponded to the hydrophobic part in the F127 surfactant micelle and the newly appeared small pores (2.67 nm) were due to the removal of the silica. The measured micro and mesopore volume and surface area are listed in

[a] *Green Chemical Technology Division, Korea Research Institute of Chemical Technology (KRICT) & University of Science and Technology (UST), Daejeon 305-600, Korea. E-mail: yoonshun@krict.re.kr; Fax: +82-42-860-7381; Tel: +82-42-860-7199*
[b] *Department of Chemical Engineering, Pohang University of Science and Technology, Kyungbuk 790-784, Korea*

† Electronic supplementary information (ESI) available: Synthesis scheme (Fig. S1). XRD results (Fig. S2), TEM images (Fig. S3), elemental analysis (Fig. S4) and rate capability profiles (Fig. S5) for the two electrode materials. See DOI: 10.1039/c1cc10539f

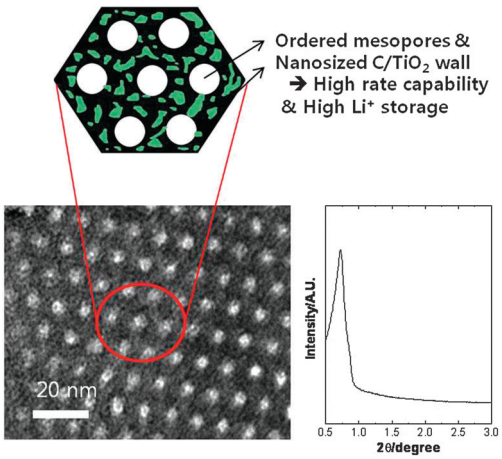

Fig. 1 Schematic explanation of a mesoporous carbon–silica–titania nanocomposite for the application as anode material in lithium ion batteries. TEM and small angle XRD show a highly ordered structure.

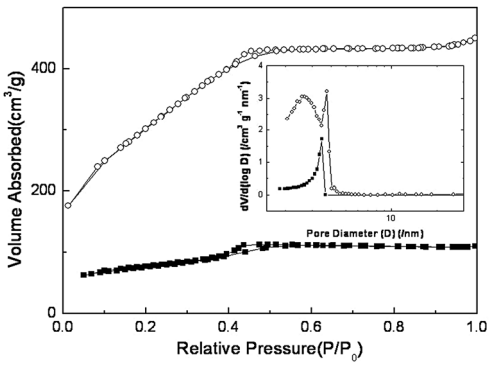

Fig. 2 N_2 sorption isotherms for m-CST (filled-rectangle) and m-CT (circle). The inset is the BJH pore size distribution calculated from the adsorption branch.

Table 1 and they increased substantially after NaOH etching. Fig. S2 (ESI†) displays the small angle and wide angle X-ray diffraction (XRD) patterns. From the small angle XRD patterns, a highly ordered structure of hexagonally pore packing was observed in the case of m-CST, but m-CT exhibited a collapsed pore structure with a low intensity ordering peak, which is indicative of collapsed pore ordering. From the wide angle XRD pattern, also, no peaks associated with titania or silica were observed, indicating that these metal oxides were amorphous.

Fig. S3 (ESI†) shows the TEM images of m-CST and m-CT. As can be seen, highly ordered mesopores appeared in m-CST and no nanosized crystals within the pore walls were observed, indicating that amorphous silica and titania were embedded within the carbon walls. This result coincided with the wide angle XRD patterns in Fig. S2 (ESI†). Using EDX for point and area analysis, carbon, Ti and Si were located homogeneously within the ordered structures in m-CST, which again confirmed that Ti and Si were homogeneously embedded within the carbon walls (see Fig. S4, ESI†). In the previous literatures, small sized crystals of titania were observed after high temperature heat treatment.[8] In our preparation, however, a silicate was added in order to reinforce the wall structure and titanium–citrate complex was employed as a Ti precursor, which resulted in the formation of amorphous TiO_2.[8]

Since an amorphous titania structure seems preferable for anode application in LIBs, the anode performances of m-CST and m-CT were investigated. In the TEM image of m-CT, furthermore, wormhole-like pores were observed, which coincided with the small angle XRD results. Using the TGA and ICP analyses of m-CST and m-CT, the carbon (C), TiO_2 and SiO_2 contents were calculated and are listed in Table 1.

Fig. 3 shows the galvanostatic charge–discharge profiles of the m-CST and m-CT electrodes. The electrodes fabrication condition was included in the ESI.† Because silica is electrochemically inactive for Li^+ storage, the contributions to the anode capacity from carbon and titania were considered and the specific capacities per unit weight of the electrochemically active materials (C_{d_a}) were compared for two electrodes.[9] No characteristic plateau associated with crystalline TiO_2 was observed in the charge–discharge profiles, as in the case of the electrode with a less-crystalline TiO_2 structure.[5] Furthermore, the disappearance of the characteristic plateau for Li^+ storage in TiO_2 has been observed in other reports when OMC composites with CoO and NiO were used as anodes.[3] Hence, this interesting profile behavior is probably related to the amorphous structure and complete nanocomposite formation. Charging capacity of m-CST and m-CT electrodes were 875 and 1405 mAh g^{-1}, respectively. By considering the electrochemically active materials, a similar charging

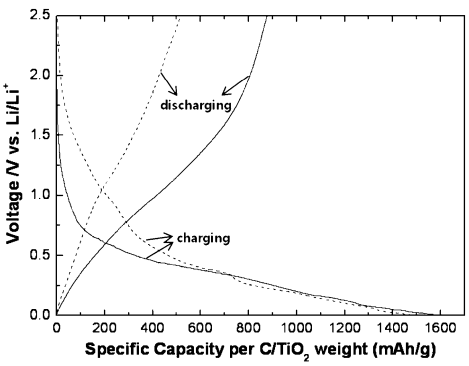

Fig. 3 The galvanostatic charge–discharge voltage profiles recorded for m-CST (solid line) and m-CT (dashed line) electrodes at 0.1 C rate.

Table 1 The physical parameters and supercapacitor properties of the b-WO_{3-X}, m-WO_{3-X} and m-WO_3 tungsten oxide electrodes

	V_{mi}/cm^3 g^{-1}	V_{me}[a]/cm^3 g^{-1}	A_{BET}[b]/m^2 g^{-1}	C/wt%	TiO_2[c]/wt%	C_d[d]/mAh g^{-1}	C_{d_a}[e]/mAh g^{-1}	IE[f]/%	Rate[g]/%
m-CST	0.03	0.14	265	44	12	490	875	56	68
m-CT	0.17	0.52	1142	84	11	492	518	35	46

[a] The micropore (V_{mi}) and mesopore (V_{me}) volume from the N_2 sorption experiment using a t-plot. [b] The surface area calculated by the BET method. [c] The carbon and TiO_2 contents are obtained by TGA and ICP experiments. [d] The specific discharge capacity measured from the initial discharge profiles. [e] The specific capacity per active material (C_d/weight fraction (C + TiO_2)). [f] The initial efficiency of the first charge–discharge capacity. [g] The rate capacity calculated by dividing the discharge capacity at 0.5 C by 0.1 C.

capacity of about 1500 mAh g^{-1} was observed for both electrodes, which was probably attributed to a higher lithium storage site in m-CST and a larger decomposition of the electrolyte in m-CT. However, the m-CST electrode showed a large C_{d_a} of 875 mAh g^{-1} and a high initial efficiency (IE) of 56%, which are much higher than those of anodes composed of OMC composites with crystalline TiO_2.[4] As regards the pure OMC anode, it was reported that tri-constituent OMC exhibited a low IE of about 30% and a high C_d of 1000 mAh g^{-1} due to its very high surface area (2390 m^2 g^{-1}) with high microporosity.[6] In contrast, OMC with a relatively low surface area of less than 1500 m^2 g^{-1} showed a low C_d value of less than 400 mAh g^{-1} and its IE remained low (about 30%). Even when OMC nanocomposites with metal oxides such as SnO_2, NiO and CoO were used, which are more highly capacitive than TiO_2, a C_d of about 600 mAh g^{-1} and IE below 50% were observed.[4] Although the exact reasons for these results remain to be elucidated, our m-CST electrode showed a high reversible capacity and good IE. Possibly, this high anode performance was due to its low surface area of 265 m^2 g^{-1} and the presence of amorphous TiO_2.

For the m-CT electrode, however, a large decrease of C_{d_a} and IE to 518 mAh g^{-1} and 35%, respectively, was observed. In this case, NaOH etching removed most of silica with 5% remaining and also dissolved some of the titania. The ratio of carbon to titania (C/TiO_2) changed from 3.6 to 7.63, indicating that a large amount of TiO_2 was lost during the NaOH etching. As shown in Fig. S2(b) (ESI†), furthermore, a slight intensity decrease of the carbon peak was observed in the case of m-CT. Hence, the large capacity loss in the m-CT electrode was probably due to the large loss of amorphous TiO_2 and the structural collapse of carbon. Furthermore, m-CT with a high surface area can give rise to more decomposition of the electrolyte, resulting in a lower IE.

Fig. 4 shows the rate capability and cyclability of the two electrodes. As can be seen, higher rate capability was observed in the case of the m-CST electrode. Note that direct comparison with other results in the literatures is difficult, because the electrode loading and its fabrication condition differ from those in previous studies. Only the comparison between m-CST and m-CT is therefore meaningful. Because the wall thickness remained invariant, the solid state diffusion length was identical for the m-CST and m-CT electrodes. Hence, the higher rate capability of m-CST was attributed to its well-ordered mesopores, which allow for the fast transport of Li^+ ions. This result is similar to that in the literature.[5,10] In Fig. 4(b), the change in the discharge capacity was plotted against the number of cycles. Although a gradual decrease in capacity was observed in the case of m-CST, the capacity became stable after 10 cycles and still remained much higher than that of the m-CT electrode. In the previous reports, the crystalline TiO_2 electrode exhibited a large capacity decrease from 300 to 200 mAh g^{-1} during initial cycling.[4,5] Because m-CST contained a small amount of amorphous TiO_2, its capacity decreased less. Hence, the better cyclability of m-CT is reasonable.

In conclusion, ordered mesoporous carbon–silica–titania was prepared by the tetra-constituent co-assembly method. Because of the potentially strong interaction between the silicate and titanate, amorphous TiO_2 embedded within the pore walls was obtained. A higher capacity, better initial efficiency and improved rate capability were observed in the case of the composite materials, due to their ordered mesoporosity and amorphous nature.

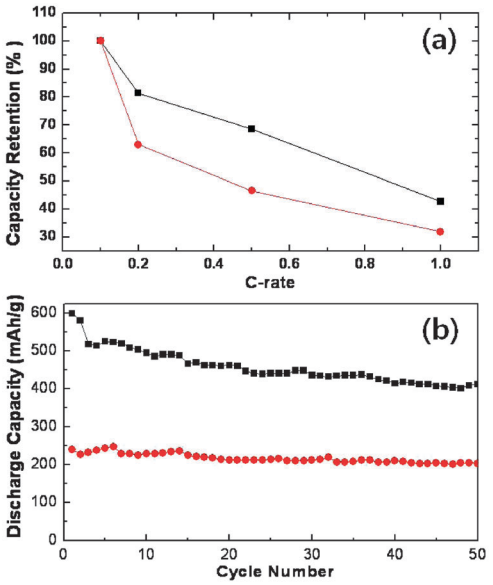

Fig. 4 (a) Rate capability from 0.1 to 1 C rate and (b) cycle performance at 0.5 C rate of m-CST (rectangle) and m-CT (circle) electrodes.

Notes and references

1 Y. Shi, B. Guo, S. A. Corr, Y.-S. Hu, K. R. Heier, L. Chen, R. Seshadri and G. D. Stucky, *Nano Lett.*, 2009, **9**, 4215; F. Jiao and P. G. Bruce, *Adv. Mater.*, 2007, **19**, 657; Y.-S. Hu, L. Kienle, Y.-G. Guo and J. Maier, *Adv. Mater.*, 2006, **18**, 1421; F. Jiao, K. M. Shaju and P. G. Bruce, *Angew. Chem., Int. Ed.*, 2005, **44**, 6550; F. Jiao, J. Bao, A. H. Hill and P. G. Bruce, *Angew. Chem., Int. Ed.*, 2008, **47**, 9711; J. Lee, M. C. Orilall, S. C. Warren, M. Kamperman, F. J. DiSalvo and U. Wiesner, *Nat. Mater.*, 2008, **7**, 222; S. C. Warren, L. C. Messina, L. S. Slaughter, M. Kamperman, Q. Zhou, S. M. Gruner, F. J. DiSalvo and U. Wiesner, *Science*, 2008, **320**, 1748.

2 P. Poizot, S. Laruelle, S. Grugeon, L. Dupont and J.-M. Tarascon, *Nature*, 2000, **407**, 496; M. Dolle, P. Poizot, L. Dupont and J.-M. Tarascon, *Electrochem. Solid-State Lett.*, 2002, **5**, A18; P. Poizot, S. Laruelle, S. Grugeon, L. Dupont and J.-M. Tarascon, *Ionics*, 2000, **6**, 321.

3 H. Zhang, H. Tao, Y. Jiang, Z. Jiao, M. Wu and B. Zhao, *J. Power Sources*, 2010, **195**, 2950; M.-Y. Cheng and B.-J. Hwang, *J. Power Sources*, 2010, **195**, 4977; G.-L. Xu, S.-R. Chen, J.-T. Li, F.-S. Ke, L. Huang and S.-G. Sun, *J. Electroanal. Chem.*, 2010, DOI: 10.1016/j.jelechem.2010.11.029.

4 L. J. Fu, H. Liu, H. P. Zhang, C. Li, T. Zhang, Y. P. Wu and H. Q. Wu, *J. Power Sources*, 2006, **159**, 219; Y. Ishii, Y. Kanamori, T. Kawashita, I. Mukhopadhyay and S. Kawasaki, *J. Phys. Chem. Solids*, 2010, **71**, 511; H. Huang, W. K. Zhang, X. P. Gan, C. Wang and L. Zhang, *Mater. Lett.*, 2007, **61**, 296.

5 D.-H. Lee, J.-G. Park, K. J. Choi, H.-J. Choi and D.-W. Kim, *Eur. J. Inorg. Chem.*, 2008, 878; S. Yoon, B. H. Ka, C. Lee, M. Park and S. M. Oh, *Electrochem. Solid-State Lett.*, 2009, **12**(2), A28.

6 H.-Q. Li, R.-L. Liu, D.-Y. Zhao and Y.-Y. Xia, *Carbon*, 2007, **45**, 2628.

7 R. Liu, Y. Shi, Y. Wan, Y. Meng, F. Zhang, D. Gu, Z. Chen, B. Tu and D. Zhao, *J. Am. Chem. Soc.*, 2006, **128**, 11652; R. Liu, Y. Ren, Y. Shi, F. Zhang, L. Zhang, B. Tu and D. Zhao, *Chem. Mater.*, 2008, **20**, 1140.

8 T. Yu, Y. Deng, L. Wang, R. Liu, L. Zhang, B. Tu and D. Zhao, *Adv. Mater.*, 2007, **19**, 2301.

9 J. O. Besenhard, *Handbook of battery materials*, Wiley-VCH, 1999.

10 S. Yoon, J. Lee, T. Hyeon and S. M. Oh, *J. Electrochem. Soc.*, 2000, **147**, 2507; J. Lee, S. Yoon, S. M. Oh and T. Hyeon, *Adv. Mater.*, 2000, **12**, 359; J. Lee, S. Yoon, S. M. Oh and T. Hyeon, *Chem. Commun.*, 1999, 2177.

